

Elastic constants of borocarbides. New approach to acoustic measurement technique

E. A. Masalitin, V. D. Fil, K. R. Zhekov, A. N. Zholobenko, and T. V. Ignatova
*B. Verkin Institute for Low Temperature Physics and Engineering,
 National Academy of Sciences of Ukraine, pr. Lenina 47, 61103 Kharkov, Ukraine*

Sung-Ik Lee

Department of Physics, Pohang University of Science and Technology, Pohang 790-784, Korea

(Dated: Published Low Temp. Phys. **29**, No. 1 (2003))

A new version of the phase method of determining the sound velocity is proposed and implemented. It utilizes the “Nonius” measurement technique and can give acceptable accuracy ($\leq 1\%$) in samples of submillimeter size. Measurements of the sound velocity are made in single-crystal samples of the borocarbides RNi_2B_2C ($R = Y, Lu, Ho$). The elastic constants and the Debye temperature are calculated.

PACS numbers:

1. INTRODUCTION

An important problem of physical acoustics is to obtain reliable data on the elastic constants of newly synthesized compounds. These data, while being of independent interest, also serve as tests for theoretical calculations of band structures, force constants, and phonon spectra. As a rule, newly synthesized materials come either in the form of products of solid-phase synthesis (i.e., more or less porous ceramics) or in the form of fine single crystals. Objects of the first group are characterized by appreciable scattering of elastic vibrations, making it practically impossible to use some version of a resonance or quiresonance (of the long-pulse type) method to determine the absolute values of the sound velocity in them. Single crystals most often are of millimeter or submillimeter size; besides, in layered crystals the characteristic size in the direction perpendicular to the layers is often 100–200 μm or even less. To determine the elastic constants of such objects the method of ultrasonic resonance spectroscopy[1] was developed, which consists in measurement of the spectrum of resonance frequencies of a sample and subsequent solution of the inverse problem of recovering all the components of the tensor of elastic constants. The technique is inherently a resonance method, i.e., it applies only to objects with small scattering (damping), a condition which is not always possible to satisfy even in small single crystals, e.g., near points of phase transitions. In addition, it can be implemented only in samples having a definite simple geometric shape (rectangular parallelepiped). The lucidity of this method is compromised by the complexity of the mathematical processing, making it hard to spot possible errors.

We have implemented a new version of the phase method of measuring sound velocities; it is applicable both to ceramic samples with strong scattering and to single crystals of submillimeter size. Utilizing a kind of “Nonius” measurement procedure, the method permits one to achieve acceptable accuracy (as a rule, better than 1%) in both cases. It has been used to measure the sound velocity in MgB_2 polycrystals[2] and in VSe_2 layered single crystals.[3] Furthermore, being completely independent of the nature of the signals to be analyzed, the instrumental implementation of the method enables one to study the variation of the amplitude and phase of any pulsed high-frequency signals. In particular, it has been used to measure the characteristics of an electric field accompanying a longitudinal sound wave in a metal.[4]

Section 2 of this paper is devoted to a description of the basic principles of implementation of the “Nonius” method of phase measurements of sound velocity. In Sec. 3 we present the results of measurements of the elastic constants in single crystals of the borocarbides RNi_2B_2C ($R = Y, Lu, Ho$).

2. “NONIUS” METHOD OF SOUND VELOCITY MEASUREMENT. PRINCIPLES AND INSTRUMENTAL IMPLEMENTATION

A block diagram of a device implementing the technique is presented in Fig. .

It is essentially a standard compensation or bridge circuit, depending on the algorithm used for process the pulsed signals, which is set by the pulse code modulation unit. In the bridge mode the signal that passed the sample channel is summarized with the equal in absolute value antiphase comparison one. The amplitude and phase of the latter are regulated by the receiver, which functions as a null device. The unbalance signal is separated into amplitude and phase components by high-frequency synchronous detectors.[5] In the compensation mode the receiver, with the aid

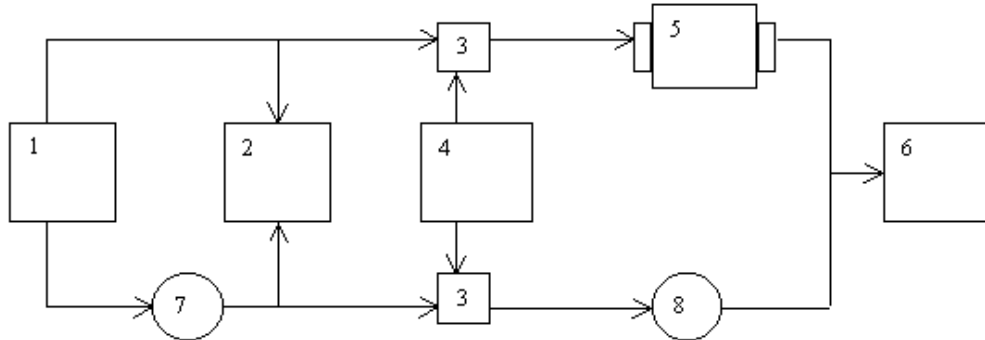


FIG. 1: Block diagram of the instrument: 1 — frequency synthesizer, 2 — phase meter, 3 — switches, 4 — pulse-code modulation unit, 5 — sample with piezotransducers, 6 — receiver, 7 — electronically tunable phase shifter, 8 — smoothly adjustable attenuator.

of sampling-storage devices, matches the amplitudes of the signals arriving at its input at different times. In this case the unbalance signals with respect to amplitude and phase are produced through a special code modulation of the pulse trains of the signals in the two channels. In any variant the data input to the computer are the readings of an attenuator (amplitude of the comparison signal) and phase meter (phase difference of the signal to be analyzed and the comparison signal).

Two original developments employed in the implementation of this standard scheme have substantially expanded its operational capabilities: an electronically controlled (linear) phase shifter with a practically unlimited tuning range, and a new data processing algorithm, which maintains a phase shift of 120° (or 240°) between the signals being analyzed. The advantages of the new phase shifter are quite obvious. In particular, in relative measurements this phase shifter provides a practically unlimited dynamic range while maintaining an extremely high accuracy of measurement, which is actually determined by the resolution of the phase meter (at a signal-to-noise ratio ≥ 5). Let us discuss the second development in somewhat more detail. In the bridge mode the working algorithm of the circuit consists in maintaining a null signal at the input of the receiver upon changes in the sound velocity and damping in the sample. In inhomogeneous (e.g., polycrystalline) samples, internal re-reflections and mutual conversion of different modes at inhomogeneities lead to nonconstancy of the phase of the signal over the duration of the rf pulse envelope. The same situation is observed in short single crystals due to the superposition of secondary reflections. In this case the length of the time interval during which the sum of the two signals has zero amplitude turns out to be short ($\leq 10^{-7}$ s). For analysis of such narrow features the receiving system should have a rather wide passband and not allow any overshoots under reproducing steep signal fronts.

For the 120° algorithm the sum of two signals of identical amplitude (their equality is maintained by an independent channel) is equal to the amplitude of each of the signals (equilateral triangle). In this case at the time of sampling-storage there are no sharp amplitude drops at the input of the receiver; this substantially improves the working of the system as a whole. A distinct advantage of the 120° algorithm is that it is unnecessary to have frequency (phase) modulation of the master oscillator in order to obtain unbalance signals of different polarity upon passage through the compensation point, as one must have for self-balancing of the circuit. Furthermore, the usual amplitude detection

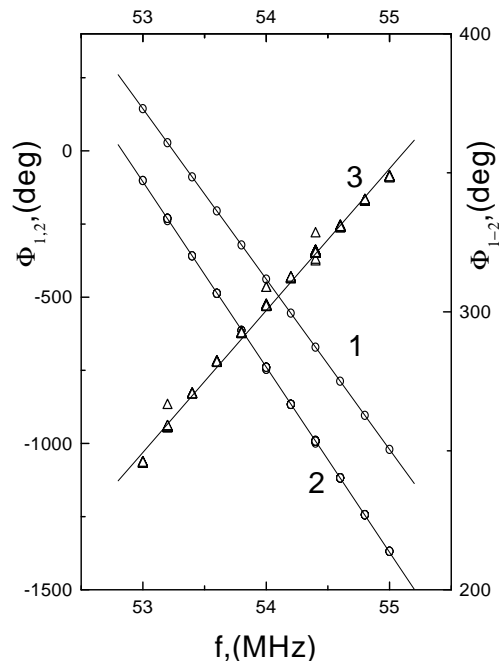


FIG. 2: Phase–frequency characteristics of the delay lines (1), of a sandwich consisting of the sample (LuNi₂B₂C, $\mathbf{q} \parallel [100]$, $\mathbf{u} \parallel [100]$, $L = 0.835$ mm) and the delay lines (2), and the difference function, i.e., the P–F characteristic of the sample (3). Note the difference in the scales of the vertical axes.

used in the 120° algorithm allows one to use as the signals of the two channels any two reflections that have traveled different distances in the sample.

The measurement algorithm in part resembles one proposed earlier.[6] First the phase–frequency (P–F) characteristic of an acoustic circuit consisting of two delay lines is measured at fixed frequency points (step 1). Then the P–F characteristic of a sandwich consisting of the same delay lines but with the sample between them (Fig. 2) is measured at the same temperature (step 2).[11]

Because the signal circuits contain elements capable of resonating (piezotransducers, imperfectly matched feeders), each of these characteristics is not necessarily a straight line. However, their difference, i.e., the P–F characteristic of the sample, in the absence of interference distortions in it, should form a strictly straight line, the slope of which determines the phase velocity of the sound,

$$v = \frac{360L}{S} \quad (1)$$

where v is the sound velocity (cm/s), L is the thickness of the sample (cm), and S is the slope of the P–F difference characteristic (deg/Hz). It is easily seen by a direct calculation that when the P–F characteristics 1 and 2 are approximated by straight lines by the least-squares method (the slopes are S_1 and S_2 , respectively), then

$$S = S_1 - S_2 \quad (2)$$

for any deviations of the P–F characteristics 1 and 2 from straight lines. This relation is valid only if the frequency points at which the P–F characteristics 1 and 2 are measured are coincident. In Ref. 6 essentially the same procedure was used to determine S , but since the technique used there did not guarantee the required coincidence, additional errors could have been introduced.

If S is comparable to S_1 (0.3 or larger), then in homogeneous materials the measurements can be limited to this step with completely acceptable accuracy (0.3% or better).

However, in homogeneous but rather thin samples the superposition of secondary reflections distorts the main part of the measurement signal. Because of this, the parts of the pulse that coincide with the leading edge are customarily

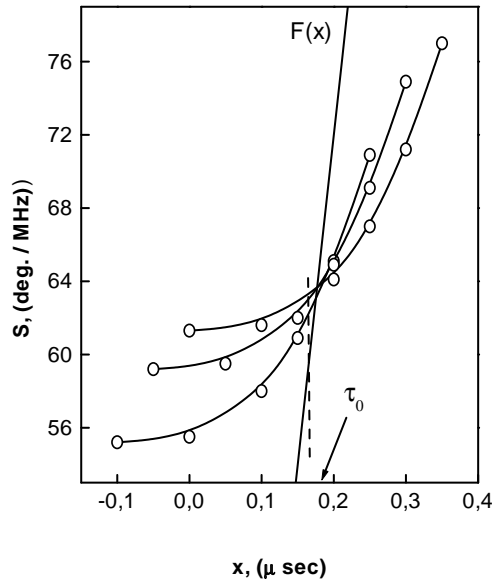


FIG. 3: Example of the interpolation procedure for finding the sound delay time τ_0 . $\text{YNi}_2\text{B}_2\text{C}$ sample ($\mathbf{q} \parallel [100]$, $\mathbf{u} \parallel [010]$, $L = 0.885$ mm) for several values of t_c (see text). At $x = 0$ the values of t_c increase from bottom to top with a step of 5×10^{-8} s. The linear function $F(x) = 360x$.

used for measurements. An analogous procedure, as a rule, should be used in inhomogeneous materials for the reasons already mentioned, even though the acoustic path length in them may be comparatively large.

As a result of the occurrence of various kinds of transient processes, the rate of which depends on the carrier frequency of the pulses, the slopes of the P–F characteristics 1 and 2 become functions of the temporal position of the strobe readout pulse at the leading edge of the measurement signal. The variation of $S_{1,2}$, depending on the type of piezotransducers, is 2–4% (for comparison, in extended samples the variation of $S_{1,2}$ at the steady part of the pulse is at the 0.1% level). This means that in going from step 1 to step 2 the readout pulse should be shifted precisely by the sound delay time τ_0 in the sample. Since the latter is initially unknown and also because of the discreteness of the step for the time shift of the strobe signal (5×10^{-8} s in our experiments), it was practically impossible to satisfy this condition. For finding τ_0 (and, hence, the sound velocity) we used the following interpolation procedure.

For each series of measurements with a definite mode (longitudinal or transverse) we calibrated the dependence of S_1 on the temporal position t_x of the readout pulse. Then for a given sample we measured S_2 at some known position t_c of the readout pulse at the leading edge of the signal. It is easy to see from Eqs. (1) and (2) that τ_0 is a solution of the equation $S(x) = 360x$, where $x \equiv t_c - t_x$ is the time shift of the readout pulse between the set of calibration measurements S_1 and the measurements with the sample, S_2 . An example of the graphical solution of the interpolation equation for several values of t_c is presented in Fig. 3. The results of the interpolation (the value of τ_0) coincide regardless of the choice of t_c .

At this step of the procedure the “rough” determination of the sound velocity is completed. To refine the values we use the “Nonius” method. Let the phase of the signal registered at some definite frequency f_0 by the phase meter in step 1 be equal to Φ_1 . In step 2 at the same frequency the phase of the signal will be Φ_2 . The total phase inserted by the sample is $\Phi_0 = 360n + (\Phi_2 - \Phi_1)$, where $n = 0, 1, 2, \dots$. Since $\Phi_0 = 360f_0L/v$, by trying values of n we find the refined value of v that is closest to the “rough” estimate.

In the above discussion it was tacitly assumed that on going from step 1 to step 2 the phase of the signal changes only because of the addition of the sample. Actually, however, besides the sample we also had an additional layer of grease in step 2. During measurements in very thin samples the contribution of the grease layer can become noticeable. In our experiments GKZh-94 silicone oil was used as the bonding agent, forming a layer $\sim 1\text{--}2$ μm thick

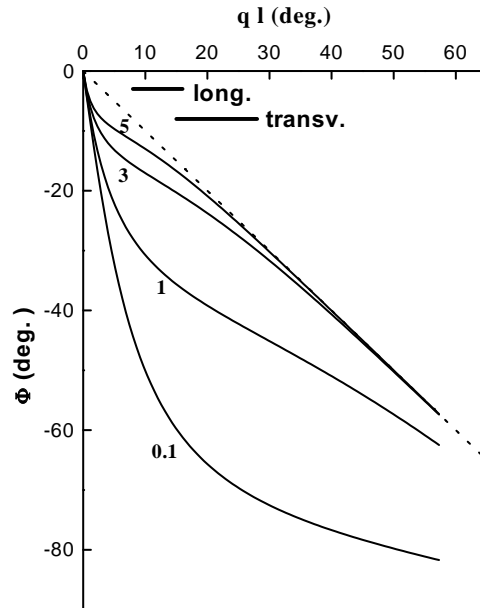


FIG. 4: Diagram pertaining to the calculation of the additional phase shift inserted by the grease layer. The reflection coefficient at the grease-sample boundary $k = 0.85$, and the numbers on the curves give the sound damping coefficient in the grease layer (neper/cm). The dotted curve corresponds to $\Phi = -ql$. The horizontal lines indicate the regions of the actual values of the parameter ql for the corresponding mode.

between the ground surfaces. The passage of an elastic wave through such a thin layer is described by the sum of an infinite geometric progression with the denominator $q = k^2 e^{-2l(\alpha+iq)}$, where k is the reflection coefficient at the boundary (we assume that the wave impedances of the delay line and sample are close in value), l is the thickness of the grease layer, α is the damping coefficient, and q is the wave number.

An estimate of the propagation velocity of sound in the grease gave $v_l \sim 2.1 \times 10^5$ cm/s, $v_t \sim 1.2 \times 10^5$ cm/s, which correspond to reflection coefficients $k \sim 0.85$ for our samples. In Fig. 4 we present the calculated dependence of the phase of the wave passing through the grease layer on the thickness for various damping coefficients. The regions of ql corresponding to the conditions of the experiment are also indicated in Fig. 4.

At low damping the correction can be rather large. We were unable to estimate the value of the sound damping in the grease — in thick layers (~ 0.5 mm) it was very large, probably because of cracking — but we assume that its value is found at the 20 dB/cm level or higher, i.e., the phase inserted by the grease layer is close to ql . In processing the results of the measurements we introduced a correction for the additional grease layer — 10° for longitudinal sound and 20° for transverse sound. In thin samples the effect of this correction was not over 1%. We suppose that this correction can be eliminated by making comparative measurements on two samples of different thickness.[3] In that case the length difference δL should be comparable to L , since otherwise the contribution of possible nonuniformities of the sound velocity over the whole length of the sample would be attributed to the small difference δL .

Let us conclude with an estimate of the potential accuracy of a single measurement. Special studies have established that the irreducibility of the phase upon the remounting (regluing) of the acoustic circuit is at the level of 20° . We estimate the indeterminacy of the correction for the additional grease layer to be 10° . Assuming that the accuracy of the “rough” estimate of the velocity is sufficient for determining the necessary value of n , we obtain for the measurement error (at $f_0 \sim 50$ MHz)

$$\frac{\delta v}{v} = \frac{30}{\Phi_0} \approx 2 \cdot 10^{-9} \frac{v}{L} \quad (3)$$

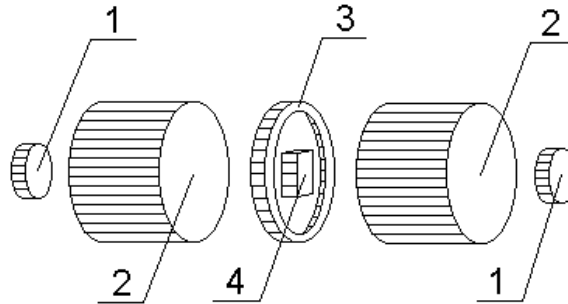


FIG. 5: Diagram of the mounting of the sample: 1 — piezotransducers, 2 — delay lines, 3 — brass support ring, 4 — sample.

3. ELASTIC CONSTANTS OF BOROCARBIDES RNi_2B_2C ($R = Y, Lu, Ho$)

In spite of the significant interest in the family of superconducting borocarbides, very little information about their elastic properties can be found in the literature. We know of only one “acoustical” study,[7] devoted to YNi_2B_2C , in which the sound velocity was measured by a time-of-flight method. Single crystals of borocarbides were grown by the method described in Ref. 8 and had the shape of a slab with a maximum dimension along the $[001]$ axis of ~ 0.8 mm ($R = Y$), ~ 0.2 mm ($R = Ho$), and ~ 0.4 mm ($R = Lu$). They were quite brittle, and therefore the mounting of the samples between the delay lines was done with the aid of a special brass ring, which acted as a holder and reinforcer; the ring was ground simultaneously with the preparation of the working faces (Fig. 5). The diameter of the ring was chosen larger than the diameter of the piezotransducers to prevent spurious signals.

All of the measurements were made at liquid nitrogen temperature. The results are presented in Table I. It contains some “superfluous” data, marked by an asterisk (*). For example, for C_{44} it was sufficient to make a single measurement $\mathbf{q} \parallel [100]$, $\mathbf{u} \parallel [001]$ (\mathbf{u} is the polarization vector of the elastic wave). We assume, however, that having the “superfluous” data will make it possible to get an idea of the accuracy of the measurements in this case.

One can also see that certain relations which follow from the general theory of elasticity[9] are well satisfied. For example, in a tetragonal crystal the sum of the squares of the velocities of the three modes remains constant under rotation of the wave vector \mathbf{q} in the (001) plane.

The elastic constants of the single crystals studied are presented in Table II. The x-ray densities were used in calculating them. For $R = Y$ the agreement with the results of Ref. 7 is poor, although the relationships among the various constants are preserved on the whole. The Debye temperature was calculated according to the formula[9]

$$\theta_D = 1146.8 \left(\frac{\rho s}{AI} \right)^{1/3} \quad (4)$$

where A is the molecular weight, s is the number of atoms in the molecule, ρ is the mass density, and I is the sum of the inverse cubes of the phase velocities of the elastic waves, averaged over all directions of the wave normal. For $R = Ho$, because of the difficulty of preparing a sample of the required orientation, the elastic constant C_{13} was not measured, and in the calculation of the bulk modulus and Debye temperature it was assumed equal to the value of C_{13} in lutecium borocarbide. For $R = Y$ the calculated value of θ_D is close to the thermodynamic estimate.[10] For $R = Lu$ the deviation of the calculated value of Θ_D from the thermodynamic value is, generally speaking, greater than the allowable error. That may be an indication of the existence in lutecium borocarbide of a low-temperature ferroelastic structural transition, accompanied by a significant softening of some elastic constant. Our preliminary measurements in holmium borocarbide have shown that at 5.2 K the velocity of the C_{66} mode falls to $\sim 3.3 \times 10^5$ cm/s. When this softening is taken into account, one obtains $\theta_D = 383$ K for $R = Ho$.

This study was partly supported by the Government Foundation for Basic Research of the Ministry of Education and Science of Ukraine (Grant No. 0207/00359).

TABLE I: Sound velocity in single crystals of borocarbides ($T = 77$ K).

Polarization		YNi ₂ B ₂ C	LuNi ₂ B ₂ C	HoNi ₂ B ₂ C
$\mathbf{q} $	$\mathbf{u} $	$v \cdot 10^5$ cm/sec	$v \cdot 10^5$ cm/sec	$v \cdot 10^5$ cm/sec
[100]	[100]	6.78 (0.885)	5.88 (0.8)	6.04 (0.606)
	[001]	3.25 (0.885)	2.65 (0.8)	2.73 (0.606)
	[010]	4.80 (0.885)	4.30 (0.8)	4.33 (0.606)
[110]	[110]*	7.55 (0.59)	6.64 (0.988)	6.86 (0.525)
	[001]*	3.26 (0.59)	2.64 (0.988)	-
	[$\bar{1}10$]	3.34 (0.59)	2.77 (0.988)	2.83 (0.525)
[001]	[001]	6.49 (0.84)	6.01 (0.4)	5.91 (0.23)
	[100]*	3.26 (0.84)	2.70 (0.4)	2.81 (0.23)
	[010]*	3.28 (0.84)	2.70 (0.4)	2.83 (0.23)
45° from the [001] axis in the (110) plane	QL*	7.28 (0.303)	-	-
	QT	3.18 (0.465)	-	-
	[110]*	3.31 (0.303)	-	-
45° from the [001] axis in the (100) plane	QT	-	2.01 (0.27)	-

TABLE II: Calculated parameters for borocarbides ($T = 77$ K)

Parameters	YNi ₂ B ₂ C		LuNi ₂ B ₂ C	HoNi ₂ B ₂ C
C_{11}	27.94	22[7]	29.39	29.47
C_{12}	14.39	9.84[7]	16.34	16.53
C_{13}	17.81		23.15	
C_{33}	25.61	21.1[7]	30.68	28.20
C_{44}	6.43	5.42[7]	5.97	6.02
C_{66}	14.00	13.1[7]	15.71	15.15
B	20.16		20.27	23
θ_D , K	501	490[10]	409 (360[10])	404
ρ , g/cm ³	6.08	6.05[7]	8.5	8.08

Note: The “superfluous” data are denoted by an asterisk (*). QL and QT are the quasilongitudinal and quasitransverse modes; the thickness of the sample in mm is given in parentheses.

Note: C_{ik} are elastic constants (in units of 10^{11} dyn/cm²), θ_D is the Debye temperature, and B is the bulk modulus. For Ho the modulus C_{13} was not measured, and in the calculation of θ_D and B it was assumed equal to 23.15 (see text).

-
- [1] A. Migliori, J. L. Sarrao, W. M. Visscher, T. M. Bell, M. Lei, Z. Fisk, and R. G. Leisure, *Physica B* **183**, 1 (1993).
[2] T. V. Ignatova, G. A. Zvyagina, I. G. Kolobov, E. A. Masalitin, V. D. Fil, Yu. B. Paderno, A. N. Bykov, V. N. Paderno, and V. I. Lyashenko, *Fiz. Nizk. Temp.* **28**, 270 (2002) [*Low Temp. Phys.* **28**, 190 (2002)].
[3] I. A. Gospodarev, A. V. Eremenko, T. V. Ignatova, G. V. Kamarchuk, I. G. Kolobov, P. A. Minaev, E. S. Syrkin, S. B. Feodos'ev, V. D. Fil, A. Soreau-Leblanc, P. Molinie, and E. C. Faolques, *Fiz. Nizk. Temp.* [*Low Temp. Phys.*] (in press).
[4] Yu. A. Avramenko, E. V. Bezuglyi, N. G. Burma, V. M. Gokhfeld, I. G. Kolobov, V. D. Fil, and O. A. Shevchenko, *Low*

Temp. Phys. **28**, 328 (2002).

- [5] V. D. Fil', P. A. Bezuglyĭ, E. A. Masalitin, and V. I. Denisenko, Prib. Tekh. Éksp., No. 3, 210 (1973).
- [6] E. V. Bezuglyĭ, N. G. Burma, I. G. Kolobov, V. D. Fil', I. M. Vitebskiĭ, A. N. Knigavko, N. M. Lavrinenko, S. N. Barilo, D. I. Zhigunov, and L. E. Soshnikov, Fiz. Nizk. Temp. **21**, 86 (1995) [Low Temp. Phys. **21**, 65 (Erratum p. 452) (1995)].
- [7] S. Isida, A. Matsushita, H. Takeya, and M. Suzuki, Physica C **349**, 150 (2001).
- [8] M. O. Mun, S. I. Lee, W. C. Lee, P. C. Canfield, B. K. Cho, and D. C. Johnston, Phys. Rev. Lett. **76**, 2790 (1996).
- [9] F. I. Fedorov, *Theory of Elastic Waves in Crystals*, Plenum Press, New York (1968), Nauka, Moscow (1965).
- [10] H. Michor, T. Holubar, C. Dusek, and G. Hilscher, Phys. Rev. B **52**, 16165 (1995).
- [11] At the frequencies we used the scale of the phase variations of the signal are much greater than 360° . The phase meter, of course, measures phase differences in the interval $0-360^\circ$, and the absence of discontinuities (360° jumps) in Fig. 2 is achieved through programming.